

Optimization of the Compressive Strength Properties of Laterite Saw-Dust Ash Sandcrete Bricks for Road Paving Applications

Habeeb Temitope Alao¹, Emmanuel E. Ndububa², Ocholuje S. Ogbo³, Balogun Samson⁴

(Civil Engineering Department, University of Abuja)

(Email: temitope.alao2019@uniabuja.edu.ng)

University of Abuja, Abuja, Nigeria

Corresponding author, Habeeb Temitope, temitope.alao2019@uniabuja.edu.ng

Abstract:

The production of Ordinary Portland Cement (OPC) is a significant source of global CO₂ emissions, driving the need for sustainable alternatives in construction materials. This study investigates the optimization of sandcrete bricks incorporating laterite soil and sawdust ash (SDA) as partial replacements for cement and fine aggregate, specifically for road paving applications. A comprehensive experimental program was executed using a Scheffé's mixture design with five components water, cement, SDA, fine aggregate, and laterite generating 35 distinct mixtures. The compressive strength of these mixtures was determined at 28 days, and the data were utilized to develop a highly accurate third-degree polynomial regression model ($R^2 = 0.9954$). The results demonstrate that optimal mixtures with moderate SDA (5-10%) and laterite (5-15%) content can achieve compressive strengths exceeding 51 MPa, comparable to conventional sandcrete. However, higher replacement levels induced a strength reduction of up to 28%, attributed to cement dilution and the deleterious effects of elevated alkali content in SDA. Computational optimization identified seven optimal mix proportions with predicted compressive strengths ranging from 32 MPa to 37 MPa, suitable for structural paving elements like kerbs and interlocking blocks. This research conclusively establishes that laterite and SDA are viable supplementary cementitious materials, but their successful application hinges on precise proportioning to leverage their pozzolanic benefits while mitigating their adverse effects, thereby offering a pathway for more eco-friendly construction in the roadway sector.

Keywords: Sustainable Construction; Sawdust Ash; Laterite; Scheffé's Optimization; Sandcrete Bricks; Compressive Strength; Road Paving.

1. Introduction

Concrete is one of the most commonly used materials in construction worldwide, valued for its durability, versatility, and strength. However, cement, the main binding agent in concrete, has a significant environmental impact. The production of Ordinary Portland Cement (OPC) is highly energy-intensive and accounts for approximately 8% of global carbon dioxide (CO₂) emissions, contributing to climate change and environmental degradation [1], [2]. With the growing demand for sustainable building materials, finding alternatives to traditional cement is becoming crucial. One promising solution is the use of Supplementary Cementitious Materials (SCMs), such as laterite and Saw Dust Ash, as partial replacements for OPC [3].

The use of SCMs in concrete has gained attention for its potential to lower the carbon footprint of concrete while maintaining or even enhancing its performance. Laterite, a soil rich in iron and aluminum, can provide beneficial properties to concrete mixtures when utilized appropriately, contributing pozzolanic activity, which reacts with calcium hydroxide in the system [4]. Similarly, Saw Dust Ash, a byproduct from the combustion of biomass, has shown promise as a partial cement replacement because of its pozzolanic nature, improving the durability and strength of concrete [5].

When produced effectively, both materials can enhance the compressive strength of concrete during the curing process and reduce the heat of hydration in large concrete pours a vital characteristic for massive constructions. Additionally, incorporating laterite helps mitigate issues such as thermal cracking, while Saw Dust Ash can improve workability and resistance to chemical attacks [6].

Laterite and Saw Dust Ash also offer economic advantages in concrete production. These materials are often sourced locally, reducing transportation costs and reliance on imported materials [7]. The use of Saw Dust Ash not only provides a solution for waste management but can also significantly reduce material costs, particularly when sourced from nearby biomass facilities [2]. Furthermore, evaluating the environmental implications of using these SCMs reveals that they can enhance the sustainability profile of concrete, contributing to the reduction of CO₂ emissions associated with traditional cement production [8].

However, integrating laterite and Saw Dust Ash into concrete mixes is not without challenges. Variations in the quality and chemical composition of these materials can lead to inconsistent concrete characteristics. Moreover, difficulties in controlling the properties of concrete at higher levels of SCM incorporation have been reported, resulting in varied mechanical properties [5], [6]. Some research shows improvements in strength and durability, while others highlight issues with early-age strength development, which is critical in certain applications [3]. Thus, ongoing research aims to identify optimal mix designs that maximize the benefits while minimizing potential drawbacks [1], [4] and address knowledge gaps regarding the long-term sustainability of these SCMs in concrete [8].

This study seeks to explore the effects of laterite and Saw Dust Ash on concrete's compressive strength while developing an optimized mix design that balances performance with environmental impact [9]. Utilizing advanced modeling approaches, including the third-degree Scheffé's polynomial optimization model, we aim to determine the ideal proportions of laterite and Saw Dust Ash that enhance mechanical performance while reducing the carbon footprint of concrete production [10]. Insights gained from this study will inform construction practices and contribute to global efforts aimed at lowering the environmental impact of construction materials.

2. Materials and Methods

2.1 Materials

The materials used in this study include Ordinary Portland Cement (OPC), Saw Dust Ash, Fine Aggregate, Laterite Soil and Potable Water. The specific properties and characteristics of each material are detailed as follows:

Ordinary Portland Cement (OPC): The OPC used was sourced from a local supplier and conformed to the standard specifications of ASTM C150. The cement was stored in dry conditions to avoid moisture.

Saw Dust Ash: Saw Dust Ash a Class C ash was obtained from local bakeries where wood materials such as firewood and saw dust are used as fuel. Saw Dust Ash as classified by ASTM C618 exhibited pozzolanic properties, due to its the presence of silica (SiO₂), alumina (Al₂O₃) and sparse quantities of Fe₂O₃. It was sieved through a 200-micrometer mesh before use to ensure consistency in particle size.

Laterite Soil: the soil sample was sourced from a borrow pit within the Abuja Municipal Area Council (AMAC) within Federal capital territory. Mineralogical characterization of the material indicates the presence of significant quantities of SiO₂, Fe₂O₃ and Al₂O₃ indicting its suitability for pozzolanic activity within concrete matrix. The sample laterite soil was air dried at room temperature and sieved through a 200-micrometer sieve to ensure uniform particle size and the removal of organic matter.

Fine Aggregate: The fine aggregate employed was river sand conforming to ASTM C33 grading requirements. It had a fineness modulus of 2.5 and was free from deleterious materials such as clay and silt.

Water: Potable water, free from impurities and meeting the requirements of ASTM C94, was used for mixing and curing the concrete.

2.2 Sample Preparation

Upon collection of sample Ordinary Portland Cement (OPC), Saw Dust Ash, Fine Aggregate, and Laterite Soil and subsequent stabilizing of these materials at room temperature to achieve stable moisture composition, the specific densities were determined subsequent to mixture design composition.



(a) Cement+Fine-Agg.+Laterite+Sawdust Ash



(b) Mixing samples



(c) Moulded sample



(d) Cured sample

As required by Scheffé's algorithm for mixture experiments comprising of 5 – mixture items for a D-Optimal mixture configuration using a third-degree polynomial, a total of 35 variant mixture were prepared for Water, Cement (OPC), Saw Dust Ash, Fine Aggregate, and Laterite Soil. This is as required by Eqn. (1.0) [11].

$$N(q, m) = \frac{(q + m - 1)!}{m! (q - 1)!} \quad (1.0)$$

where q is the number of mixture materials and m is the polynomial degree.

Five number set of practical initial trial mixtures A were developed and constituted into a mixture matrix in Eqn. (2.0) with each column comprising; water, cement, **Saw Dust Ash**, fine aggregate, and Laterite soil, respectively.

$$A = \begin{bmatrix} 0.550 & 1.000 & 0.000 & 1.500 & 0.000 \\ 0.600 & 0.950 & 0.050 & 1.450 & 0.150 \\ 0.650 & 0.900 & 0.100 & 1.200 & 0.300 \\ 0.700 & 0.850 & 0.150 & 1.050 & 0.450 \\ 0.750 & 0.800 & 0.200 & 0.950 & 0.550 \end{bmatrix} \quad (2.0)$$

Other serial real mixture design components Z were determined by Eqn (3.0) for subsequent cycles of experimental trials. Experimental mix proportions are given in Table 1.0.

$$Z = X \cdot A \quad (3.0)$$

Following the determination of Scheffé's Mixture space, laboratory mixture quantities were calculated as detailed in Table 3.0. The density values of the material were determined before mixture computations [12]. The preliminary density of the mixture samples is 1,000.00, 1,684.21, 2,669.32, 2,419.89 and 2,055.00 kg/m³ for Water, Cement, Saw Dust Ash, Fine-Aggregate, and Laterite soil respectively.

Table 3.0: Scheffé's $N(5, 3)$ Mixture points for - water, cement, **Saw Dust Ash**, fine aggregate, and Laterite soil – Lattice Tetrahedron.

| S/No. | MIXTURE POINTS | PSEUDO COMPONENT - X | | | | | REAL COMPONENTS - Z | | | | |
|-------|----------------|----------------------|------|------|------|------|---------------------|--------|--------------|-----------|----------|
| | | X1 | X2 | X3 | X4 | X5 | Z1 | Z2 | Z3 | Z4 | Z5 |
| | | | | | | | Water | Cement | Saw Dust Ash | Fine Agg. | Laterite |
| 1 | R1 | 1 | 0 | 0 | 0 | 0 | 0.550 | 1.000 | 0.000 | 1.500 | 0.000 |
| 2 | R2 | 0 | 1 | 0 | 0 | 0 | 0.600 | 0.950 | 0.050 | 1.450 | 0.150 |
| 3 | R3 | 0 | 0 | 1 | 0 | 0 | 0.650 | 0.900 | 0.100 | 1.200 | 0.300 |
| 4 | R4 | 0 | 0 | 0 | 1 | 0 | 0.700 | 0.850 | 0.150 | 1.050 | 0.450 |
| 5 | R5 | 0 | 0 | 0 | 0 | 1 | 0.750 | 0.800 | 0.200 | 0.950 | 0.550 |
| 6 | R12 | 0.5 | 0.5 | 0 | 0 | 0 | 0.575 | 0.975 | 0.025 | 1.475 | 0.075 |
| 7 | R13 | 0.5 | 0 | 0.5 | 0 | 0 | 0.600 | 0.950 | 0.050 | 1.350 | 0.150 |
| 8 | R14 | 0.5 | 0 | 0 | 0.5 | 0 | 0.625 | 0.925 | 0.075 | 1.275 | 0.225 |
| 9 | R15 | 0.5 | 0 | 0 | 0 | 0.5 | 0.650 | 0.900 | 0.100 | 1.225 | 0.275 |
| 10 | R23 | 0 | 0.5 | 0.5 | 0 | 0 | 0.625 | 0.925 | 0.075 | 1.325 | 0.225 |
| 11 | R24 | 0 | 0.5 | 0 | 0.5 | 0 | 0.650 | 0.900 | 0.100 | 1.250 | 0.300 |
| 12 | R25 | 0 | 0.5 | 0 | 0 | 0.5 | 0.675 | 0.875 | 0.125 | 1.200 | 0.350 |
| 13 | R34 | 0 | 0 | 0.5 | 0.5 | 0 | 0.675 | 0.875 | 0.125 | 1.125 | 0.375 |
| 14 | R35 | 0 | 0 | 0.5 | 0 | 0.5 | 0.700 | 0.850 | 0.150 | 1.075 | 0.425 |
| 15 | R45 | 0 | 0 | 0 | 0.5 | 0.5 | 0.725 | 0.825 | 0.175 | 1.000 | 0.500 |
| 16 | R123 | 0.33 | 0.33 | 0.33 | 0 | 0 | 0.594 | 0.941 | 0.050 | 1.370 | 0.149 |
| 17 | R124 | 0.33 | 0.33 | 0 | 0.33 | 0 | 0.611 | 0.924 | 0.066 | 1.320 | 0.198 |
| 18 | R125 | 0.33 | 0.33 | 0 | 0 | 0.33 | 0.627 | 0.908 | 0.083 | 1.287 | 0.231 |
| 19 | R134 | 0.33 | 0 | 0.33 | 0.33 | 0 | 0.627 | 0.908 | 0.083 | 1.238 | 0.248 |
| 20 | R135 | 0.33 | 0 | 0.33 | 0 | 0.33 | 0.644 | 0.891 | 0.099 | 1.205 | 0.281 |
| 21 | R145 | 0.33 | 0 | 0 | 0.33 | 0.33 | 0.660 | 0.875 | 0.116 | 1.155 | 0.330 |
| 22 | R234 | 0 | 0.33 | 0.33 | 0.33 | 0 | 0.644 | 0.891 | 0.099 | 1.221 | 0.297 |
| 23 | R235 | 0 | 0.33 | 0.33 | 0 | 0.33 | 0.660 | 0.875 | 0.116 | 1.188 | 0.330 |
| 24 | R245 | 0 | 0.33 | 0 | 0.33 | 0.33 | 0.677 | 0.858 | 0.132 | 1.139 | 0.380 |
| 25 | R345 | 0 | 0 | 0.33 | 0.33 | 0.33 | 0.693 | 0.842 | 0.149 | 1.056 | 0.429 |
| 26 | R112 | 0.66 | 0.33 | 0 | 0 | 0 | 0.561 | 0.974 | 0.017 | 1.469 | 0.050 |
| 27 | R113 | 0.66 | 0 | 0.33 | 0 | 0 | 0.578 | 0.957 | 0.033 | 1.386 | 0.099 |
| 28 | R114 | 0.66 | 0 | 0 | 0.33 | 0 | 0.594 | 0.941 | 0.050 | 1.337 | 0.149 |
| 29 | R115 | 0.66 | 0 | 0 | 0 | 0.33 | 0.611 | 0.924 | 0.066 | 1.304 | 0.182 |
| 30 | R223 | 0 | 0.66 | 0.33 | 0 | 0 | 0.611 | 0.924 | 0.066 | 1.353 | 0.198 |

| | | | | | | | | | | | |
|----|------|---|------|------|------|------|-------|-------|-------|-------|-------|
| 31 | R224 | 0 | 0.66 | 0 | 0.33 | 0 | 0.627 | 0.908 | 0.083 | 1.304 | 0.248 |
| 32 | R225 | 0 | 0.66 | 0 | 0 | 0.33 | 0.644 | 0.891 | 0.099 | 1.271 | 0.281 |
| 33 | R334 | 0 | 0 | 0.66 | 0.33 | 0 | 0.660 | 0.875 | 0.116 | 1.139 | 0.347 |
| 34 | R335 | 0 | 0 | 0.66 | 0 | 0.33 | 0.677 | 0.858 | 0.132 | 1.106 | 0.380 |
| 35 | R445 | 0 | 0 | 0 | 0.66 | 0.33 | 0.710 | 0.825 | 0.165 | 1.007 | 0.479 |

2.4 Sample Preparation Procedure

Batching and Mixing: The materials were accurately measured and mixed in the specified proportions. A mechanical drum mixer was employed to blend the water, cement, Saw Dust Ash, fine aggregate, and laterite soil for 15 minutes, ensuring a uniform and homogeneous mixture.

Concrete Casting: After mixing the dry ingredients, water was added, and blending continued for another five minutes to obtain a uniform consistency. The prepared concrete was then poured into plastic molds measuring 100 mm × 150 mm × 65 mm, designed for interlocking crib stones. Compaction was carried out using both a tamping rod and a vibrating plate to remove air pockets and ensure thorough consolidation.

Curing: The freshly poured specimens were left in the molds for 24 hours to set. After this period, the molds were removed, and the specimens were placed in a curing tank filled with clean water. The specimens were kept in the tank for 7 and 28 days, following standard curing practices.

2.5 Experimental Testing

The following tests were conducted to evaluate the mechanical properties and durability of the concrete mixtures:

Compressive Strength Test: The compressive strength of 100 mm × 150 mm × 65 mm concrete cubes was measured at 28 days of curing. A universal compression testing machine was used,

$$f_c = \frac{F}{A_c} \quad (4.0)$$

Where f_c is the compressive strength of the concrete, F is maximum load applied to the concrete specimen during the test and A_c is the cross-sectional area of the concrete specimen.

2.6 Optimization Using Scheffé's Method

The determination of the optimal mixture composition for the Saw Dust Ash and laterite soil modified Sandcrete was conducted through the application of Scheffé's third-degree polynomial model, as expressed in Eqn (5.0) and adapted to the N(5,3) mixture space [13], [14]. This model framework was selected for its suitability in capturing the interactive effects among five constituent materials water, cement, Saw Dust Ash, fine aggregate, and laterite soil which collectively define the Sandcrete mix proportions summarized in Table 3.0.

The Scheffé's third-degree polynomial model, formally presented in Eqn (6.0), was specifically tailored to represent the compressive strength response of the Sandcrete mixtures. By fitting the experimental data within this mathematical formulation, the influence and synergy of each component on the overall strength performance were effectively characterized.

Subsequently, the data fitting algorithm implemented within the Wolfram Language environment was employed to derive an optimized model representation. This computational process enabled the precise estimation of regression coefficients and the generation of response surfaces that guided the search for optimal compositions. The resulting model was further utilized for optimization analyses, executed under the boundary and constraint conditions outlined in Eqn(s) (7.0), (8.0), and

(9.0), [15] ensuring that the computed mix designs satisfied all imposed physical and compositional limitations.

$$\eta_x(X_i) = \sum_{i=1}^n \beta_i X_i + \sum_{i=1}^n \sum_{j=i+1}^n \beta_{ij} X_i X_j + \sum_{i=1}^n \sum_{j=i+1}^n \beta_{ij} X_i X_i X_j + \sum_{i=1}^n \sum_{j=i+1}^n \sum_{k=j+1}^n \beta_{ijk} X_i X_j X_k \quad (5.0)$$

Scheffé's mixture polynomial model in Eqn (6.0).

$$\begin{aligned} n(X_i) = & X_1\beta_1 + X_2\beta_2 + X_3\beta_3 + X_4\beta_4 + X_5\beta_5 + X_6\beta_6 + X_1X_2\beta_{12} + X_1X_3\beta_{13} + X_1X_4\beta_{14} \\ & + X_1X_5\beta_{15} + X_1X_6\beta_{16} + X_2X_3\beta_{23} + X_2X_4\beta_{24} + X_2X_5\beta_{25} + X_2X_6\beta_{26} \\ & + X_3X_4\beta_{34} + X_3X_5\beta_{35} + X_3X_6\beta_{36} + X_4X_5\beta_{45} + X_4X_6\beta_{46} + X_5X_6\beta_{56} \\ & + X_1^2X_2\beta_{112} + X_1^2X_3\beta_{113} + X_1^2X_4\beta_{114} + X_1^2X_5\beta_{115} + X_1^2X_6\beta_{116} + X_1X_2X_3\beta_{123} \\ & + X_1X_2X_4\beta_{124} + X_1X_2X_5\beta_{125} + X_1X_2X_6\beta_{126} + X_1X_3X_4\beta_{134} + X_1X_3X_5\beta_{135} \\ & + X_1X_3X_6\beta_{136} + X_1X_4X_5\beta_{145} + X_1X_4X_6\beta_{146} + X_1X_5X_6\beta_{156} + X_2^2X_3\beta_{223} \\ & + X_2^2X_4\beta_{224} + X_2^2X_5\beta_{225} + X_2^2X_6\beta_{226} + X_2X_3X_4\beta_{234} + X_2X_3X_5\beta_{235} \\ & + X_2X_3X_6\beta_{236} + X_2X_4X_5\beta_{245} + X_2X_4X_6\beta_{246} + X_2X_5X_6\beta_{256} + X_3^2X_4\beta_{334} \\ & + X_3^2X_5\beta_{335} + X_3^2X_6\beta_{336} + X_3X_4X_5\beta_{345} + X_3X_4X_6\beta_{346} + X_3X_5X_6\beta_{356} \\ & + X_4^2X_5\beta_{445} + X_4^2X_6\beta_{446} + X_4X_5X_6\beta_{456} + X_5^2X_6\beta_{556} \end{aligned} \quad (6.0)$$

The Scheffé's constraint, where the sum of all mixture proportion must equal unity as defined in Eqn (7.0)

$$X_1 + X_2 + X_3 + X_4 + X_5 = 1 \quad (7.0)$$

And

$$X_1; X_2; X_3; X_4 \& X_5 > 0 \quad (8.0)$$

The optimization process involves setting constraints based on the minimum and maximum acceptable values for compressive strength, ensuring that the solution satisfies the structural requirements of the concrete mix:

$$f_{min} \leq f_i(5) \leq f_{max} \quad (9.0)$$

Where f_{min} and f_{max} represent the minimum and maximum allowable strength values [11]. The number of mixture combinations required for the optimization is calculated using Eqn (9.0).

3. Results and Discussion

Mineralogical Characterization of Laterite Soil and Saw Dust Ash

As indicated in figure 1.0, the mineralogical constituents of laterite soil and Saw Dust Ash exert a considerable influence on the resultant compressive strength of sandcrete. Laterite, characterized by significant concentrations of silica (SiO_2), alumina (Al_2O_3), and iron oxide (Fe_2O_3), possesses pozzolanic potential. The silica and alumina can undergo a pozzolanic reaction with calcium hydroxide a by-product of Portland cement hydration to form secondary calcium silicate hydrate (C-S-H) and calcium aluminate hydrate phases, thereby enhancing the long-term strength and microstructural density of the composite matrix [16]. Conversely, Saw Dust Ash is typically composed of high levels of alkali oxides, particularly potassium oxide (K_2O), alongside notable amounts of calcium oxide (CaO) [17]. The elevated alkali metal content poses a significant risk of inducing alkali-silica reaction (ASR) when combined with reactive aggregates, leading to expansive gel formation, internal cracking, and a consequent reduction in compressive strength [7]. While the calcium oxide can contribute to cementitious reactions, its beneficial effect is often counteracted by the deleterious alkalis. Therefore, the net impact on the mechanical performance of

sandcrete is a function of the synergistic and antagonistic interactions between these components; optimizing the blend is critical to leveraging the pozzolanic contribution of laterite while mitigating the chemical instability imparted by the Saw Dust Ash [18].

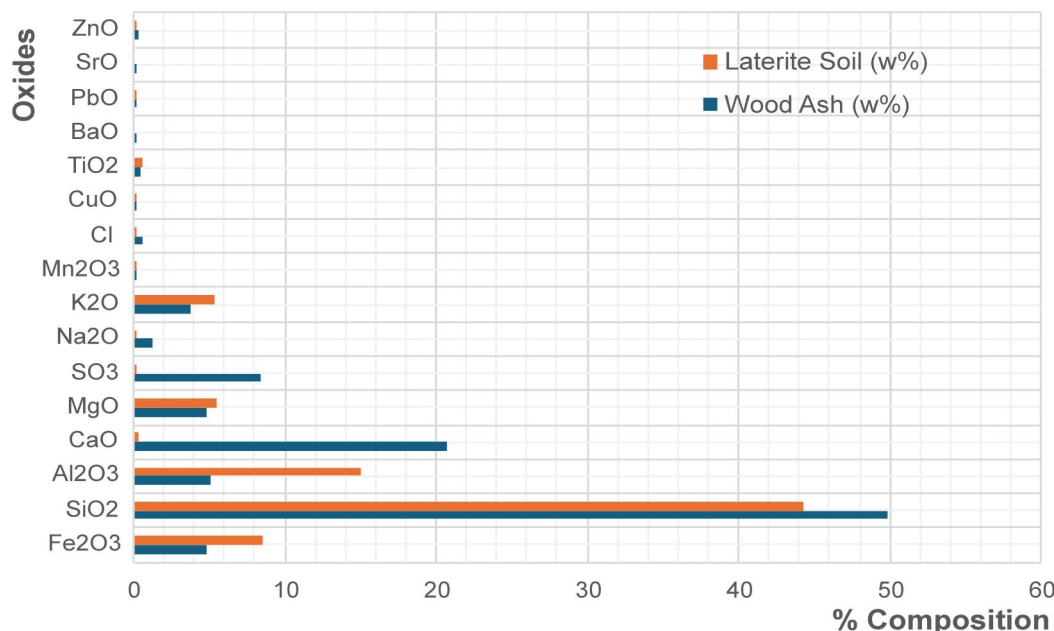


Figure 1.0: Oxide Composition of Laterite Soil and Saw Dust Ash

Efficacy of Laterite Soil and Saw Dust Ash as Partial Replacements in Sandcrete

The efficacy of incorporating laterite soil and Saw Dust Ash as sustainable partial replacements in sandcrete was evaluated through a systematic mixture design and subsequent compressive strength testing. The results, derived from a Scheffé's simplex lattice design, reveal a complex interplay between the constituent materials, where the pozzolanic potential of the additives is critically balanced against their dilutive and chemically disruptive effects.

The control mixture (R1), formulated with a conventional sandcrete composition, established a baseline compressive strength of 51.540 MPa. Notably, several modified mixtures demonstrated comparable or marginally superior performance. Specifically, mixtures R12 (51.995 MPa), R26 (51.832 MPa), and R27 (51.896 MPa) achieved optimal results. Analysis of their pseudo-component coordinates (Table 3.0) indicates that these high-performing mixes are characterized by a high proportion of the cement component (X_2) coupled with low to moderate introductions of laterite (X_5) and Saw Dust Ash (X_3). This suggests that a carefully calibrated partial replacement can leverage the supplementary cementitious properties of the additives without significantly compromising the primary hydration matrix. In these cases, the silica (SiO_2) and alumina (Al_2O_3) present in the laterite, and to a lesser extent in the Saw Dust Ash, likely participate in pozzolanic reactions with portlandite ($Ca(OH)_2$), generating secondary calcium silicate hydrate (C-S-H) phases that contribute to long-term strength development [19].

Conversely, Table 4.0 delineates a clear threshold for substitution, beyond which significant strength degradation occurs. Mixtures with elevated laterite and Saw Dust Ash content, such as R25, R12, R13, and R34, yielded the lowest mean compressive strengths, ranging from 37.077 MPa to 42.225 MPa. This decline can be attributed to a confluence of mechanisms. Primarily, the displacement of cement by less reactive materials induces a dilution effect, reducing the initial volume of primary C-S-H formed. Furthermore, the chemical composition of the Saw Dust Ash, particularly its high alkali metal oxide content (K_2O), is postulated to be a contributing factor. Elevated alkali levels can perturb the hydration kinetics and, in the presence of reactive aggregates, potentially initiate deleterious expansion mechanisms such as the alkali-silica reaction (ASR), leading to microcracking and a loss of structural integrity. The pronounced standard deviations

observed in several of these mixes (e.g., 12.912 in R16 and R21) further underscore issues of mix heterogeneity and potential inconsistency in the reactivity of the natural additives.

In synthesis, the efficacy of laterite soil and Saw Dust Ash in sandcrete is unequivocally contingent upon precise stoichiometric control. While these materials offer a viable pathway for reducing the embodied carbon of sandcrete, their application must be optimized to function as synergistic pozzolanas within a high-cement base matrix. The findings confirm that they are not direct, volume-for-volume replacements for Portland cement. Future work should focus on microstructural analysis [9], [20] to quantitatively link these compositional variations to the evolution of the hydrated phase assemblage and pore structure.

Table 4.0: Compressive Strength test responses for variation in - water, cement, **Saw Dust Ash**, fine aggregate, and Laterite soil

| S/No. | Response | Compressive Strength (MPa) | | | |
|-------|----------|----------------------------|----------|------------|--------|
| | | Trial -1 | Trial -2 | Stan. Dev. | Mean |
| 1 | R1 | 51.469 | 51.610 | 0.100 | 51.540 |
| 2 | R2 | 47.568 | 41.964 | 3.963 | 44.766 |
| 3 | R3 | 41.010 | 42.970 | 1.386 | 41.990 |
| 4 | R4 | 43.969 | 42.825 | 0.809 | 43.397 |
| 5 | R5 | 49.903 | 47.205 | 1.908 | 48.554 |
| 6 | R12 | 52.375 | 51.614 | 0.538 | 51.995 |
| 7 | R13 | 47.568 | 41.964 | 3.963 | 44.766 |
| 8 | R14 | 44.525 | 39.924 | 3.253 | 42.225 |
| 9 | R15 | 41.010 | 42.970 | 1.386 | 41.990 |
| 10 | R23 | 44.525 | 39.924 | 3.253 | 42.225 |
| 11 | R24 | 41.010 | 42.970 | 1.386 | 41.990 |
| 12 | R25 | 31.860 | 42.293 | 7.377 | 37.077 |
| 13 | R34 | 31.860 | 42.293 | 7.377 | 37.077 |
| 14 | R35 | 43.969 | 42.825 | 0.809 | 43.397 |
| 15 | R45 | 47.825 | 45.715 | 1.492 | 46.770 |
| 16 | R123 | 34.088 | 51.715 | 12.464 | 42.902 |
| 17 | R124 | 37.471 | 41.422 | 2.794 | 39.447 |
| 18 | R125 | 45.022 | 39.816 | 3.681 | 42.419 |
| 19 | R134 | 45.022 | 39.816 | 3.681 | 42.419 |
| 20 | R135 | 43.245 | 41.347 | 1.342 | 42.296 |
| 21 | R145 | 33.981 | 52.241 | 12.912 | 43.111 |
| 22 | R234 | 43.245 | 41.347 | 1.342 | 42.296 |
| 23 | R235 | 33.981 | 52.241 | 12.912 | 43.111 |
| 24 | R245 | 32.228 | 41.964 | 6.884 | 37.096 |
| 25 | R345 | 42.432 | 42.333 | 0.070 | 42.383 |
| 26 | R112 | 52.113 | 51.551 | 0.397 | 51.832 |
| 27 | R113 | 51.975 | 51.816 | 0.112 | 51.896 |
| 28 | R114 | 34.088 | 51.715 | 12.464 | 42.902 |
| 29 | R115 | 37.471 | 41.422 | 2.794 | 39.447 |
| 30 | R223 | 37.471 | 41.422 | 2.794 | 39.447 |
| 31 | R224 | 45.022 | 39.816 | 3.681 | 42.419 |
| 32 | R225 | 43.245 | 41.347 | 1.342 | 42.296 |
| 33 | R334 | 33.981 | 52.241 | 12.912 | 43.111 |
| 34 | R335 | 32.228 | 41.964 | 6.884 | 37.096 |
| 35 | R445 | 45.735 | 43.871 | 1.318 | 44.803 |

Computational Optimization of Mixture Components

In order to determine optimal mixture composition for the use of laterite soil and Saw Dust Ash in sandcrete bricks, an objective function was derived from laboratory test data given in Table 4.0.

The objective function for the compressive strength model is;

$$\begin{aligned}
 f_c(X_i) = & 51.5508X_1 + 44.77238X_2 + 19.2742X_1X_2 - 8.1498X_1^2X_2 + 41.9951X_3 \\
 & - 91.0994X_1X_3 + 165.8870X_1^2X_3 + 37.02880X_2X_3 - 43.0403X_1X_2X_3 \\
 & - 83.6728X_2^2X_3 + 43.4034X_4 - 9.0005X_1X_4 - 24.2912X_1^2X_4 \\
 & - 14.48860X_2X_4 - 150.2093X_1X_2X_4 + 11.8419X_2^2X_4 - 108.9464X_3X_4 \\
 & + 244.0587X_1X_3X_4 + 145.2794X_2X_3X_4 + 172.54310X_3^2X_4 + 48.56187X_5 \quad (10.0) \\
 & + 18.5111X_1X_5 - 101.8326X_1^2X_5 - 111.9985X_2X_5 + 39.5823X_1X_2X_5 \\
 & + 146.9077X_2^2X_5 + 63.4249X_3X_5 - 20.2025X_1X_3X_5 + 73.3213X_2X_3X_5 \\
 & - 142.2906X_3^2X_5 + 10.2863X_4X_5 - 35.7649X_1X_4X_5 - 13.1171X_2X_4X_5 \\
 & + 42.7479X_3X_4X_5 - 14.6449X_4^2X_5
 \end{aligned}$$

The coefficients β_i (for $i=1, 2, \dots, 5$) necessary for fitting Eqn. (10.0) to the compressive and flexural strength laboratory test data were determined using the "NonLinearModelFit" function in the Wolfram language. The models presented in Eqn. (6.0) and gave values of 99.54% coefficient of determination. The coefficients' values are detailed in Table 5.0. Subsequently, the developed model was utilized as the objective function in the optimization calculations.

The computation gave optimal mixture composition given in Table 6.0.

Table 5.0: Coefficients of Scheffé's Third-Degree Polynomial for Compressive Strengths for Pseudo components.

| S/No. | β_i | Estimate | Standard error | t-Statistic | P-Value |
|-------|---------------|----------|----------------|-------------|---------|
| 1 | β_1 | 51.5508 | 0.436 | 118.1090 | 0.00539 |
| 2 | β_2 | 44.7724 | 0.437 | 102.5520 | 0.00621 |
| 3 | β_3 | 41.9951 | 0.437 | 96.1872 | 0.00662 |
| 4 | β_4 | 43.4035 | 0.437 | 99.4170 | 0.00640 |
| 5 | β_5 | 48.5619 | 0.437 | 111.2380 | 0.00572 |
| 6 | β_{12} | 19.2742 | 9.674 | 1.9925 | 0.29613 |
| 7 | β_{13} | -91.0995 | 9.676 | -9.4145 | 0.06737 |
| 8 | β_{14} | -9.00059 | 9.674 | -0.9304 | 0.52294 |
| 9 | β_{15} | 18.5111 | 9.670 | 1.9142 | 0.30648 |
| 10 | β_{23} | 37.0288 | 9.661 | 3.8330 | 0.16247 |
| 11 | β_{24} | -14.4886 | 9.656 | -1.5006 | 0.37423 |
| 12 | β_{25} | -111.999 | 9.649 | -11.6076 | 0.05471 |
| 13 | β_{34} | -108.946 | 9.649 | -11.2909 | 0.05624 |
| 14 | β_{35} | 63.425 | 9.641 | 6.5783 | 0.09604 |
| 15 | β_{45} | 10.2864 | 9.648 | 1.0662 | 0.47962 |
| 16 | β_{123} | -43.0404 | 24.925 | -1.7268 | 0.33417 |
| 17 | β_{124} | -150.209 | 24.913 | -6.0293 | 0.10463 |
| 18 | β_{125} | 39.5823 | 24.903 | 1.5894 | 0.35751 |
| 19 | β_{134} | 244.059 | 24.891 | 9.8051 | 0.06470 |
| 20 | β_{135} | -20.2026 | 24.882 | -0.8119 | 0.56584 |
| 21 | β_{145} | -35.7649 | 24.901 | -1.4363 | 0.38719 |
| 22 | β_{234} | 145.279 | 24.600 | 5.9056 | 0.10679 |

| | | | | | |
|----|---------------|----------|--------|---------|---------|
| 23 | β_{235} | 73.3214 | 24.595 | 2.9811 | 0.20604 |
| 24 | β_{245} | -13.1172 | 24.623 | -0.5327 | 0.68839 |
| 25 | β_{345} | 42.7479 | 24.543 | 1.7418 | 0.33180 |
| 26 | β_{112} | -8.14982 | 16.896 | -0.4824 | 0.71388 |
| 27 | β_{113} | 165.887 | 16.899 | 9.8163 | 0.06463 |
| 28 | β_{114} | -24.2912 | 16.896 | -1.4377 | 0.38690 |
| 29 | β_{115} | -101.833 | 16.891 | -6.0287 | 0.10465 |
| 30 | β_{223} | -83.6728 | 16.877 | -4.9577 | 0.12671 |
| 31 | β_{224} | 11.8419 | 16.870 | 0.7019 | 0.61037 |
| 32 | β_{225} | 146.908 | 16.860 | 8.7133 | 0.07274 |
| 33 | β_{334} | 172.543 | 16.860 | 10.2337 | 0.06201 |
| 34 | β_{335} | -142.291 | 16.849 | -8.4451 | 0.07503 |
| 35 | β_{445} | -14.645 | 16.859 | -0.8687 | 0.54467 |

These results validate the derived models as effective tools for predicting the compressive strength characteristics of the Saw Dust Ash and laterite soil modified Sandcrete. Optimal mixture composition of the production of modified bricks are given in Table 7.0.

Table 6.0: Parameter ANOVA of Scheffé's Simplex lattice Third Degree Polynomial for Compressive Strengths for Pseudo – Components

| Parameters | Compressive Strength | | |
|-------------------|----------------------|----------|---------|
| | DF | SS | MS |
| Model | 35 | 67634.6 | 1932.42 |
| Error | 1 | 0.190644 | 0.19064 |
| Uncorrected Total | 36 | 67634.8 | |
| Corrected Total | 35 | 551.915 | |

Table 6.0: Optimal Mixture Composition for the Production of Saw Dust Ash and laterite soil modified Sandcrete Bricks.

| Mixture Item | X_i | Mix-1 | Mix-2 | Mix-3 | Mix-4 | Mix-5 | Mix-6 | Mix-7 |
|----------------------|----------|-------|-------|-------|-------|-------|-------|-------|
| Water | 0.69093 | 0.667 | 0.617 | 0.692 | 0.624 | 0.671 | 0.594 | 0.671 |
| Cement | 0.29306 | 0.883 | 0.933 | 0.858 | 0.911 | 0.863 | 0.940 | 0.863 |
| Saw Dust Ash | 0.00996 | 0.117 | 0.067 | 0.142 | 0.079 | 0.127 | 0.050 | 0.127 |
| Fines | 0.005299 | 1.186 | 1.330 | 1.109 | 1.270 | 1.135 | 1.367 | 1.141 |
| Laterite | 0.000751 | 0.334 | 0.195 | 0.409 | 0.230 | 0.366 | 0.145 | 0.368 |
| Compressive Strength | 1.0 | 35.88 | 33.13 | 37.30 | 33.51 | 36.14 | 31.89 | 36.15 |

4. Conclusion and Recommendations:

4.1 Conclusions

This study successfully demonstrates the viability and defines the optimal parameters for utilizing laterite soil and sawdust ash (SDA) as sustainable partial replacements in sandcrete bricks for road paving applications. Through a rigorous application of Scheffé's mixture design and a third-degree polynomial optimization model, the complex interactions between water, cement, SDA, fine aggregate, and laterite were systematically characterized to develop predictive models with a high coefficient of determination ($R^2 = 0.9954$).

The key findings of this investigation are threefold.

1. The mineralogical composition of the additives plays a critical role; the pozzolanic silica and alumina in laterite contribute to secondary strength-forming reactions, while the high alkali content (K₂O) in SDA presents a potential risk for durability issues at elevated replacement levels.
2. The experimental results delineate a clear threshold for substitution. While optimal mixtures with moderate SDA and laterite content (e.g., R12, R26, R27) achieved compressive strengths comparable to the conventional control mix (51.54 MPa), higher replacement levels led to significant strength reduction up to 28% in some cases primarily due to cement dilution and chemical interference.
3. The derived computational model enabled the identification of seven optimal mixture compositions, with predicted compressive strengths ranging from approximately 32 MPa to 37 MPa, validating the efficacy of the optimization approach.

4.2 Recommendations

This research establishes that laterite and SDA can be effectively valorised in the production of structural-grade sandcrete bricks, contributing to waste reduction and a lower carbon footprint in construction. However, their efficacy is strictly contingent upon precise, optimized proportioning to balance their pozzolanic benefits against their dilutive and chemically disruptive effects. The models and optimal mixes presented provide a practical framework for manufacturers. For future work, it is recommended that these findings be corroborated with long-term durability studies, including resistance to abrasion, water absorption, and sulphate attack, specifically for paving applications.

References:

- [1] E. Teixeira, R. Mateus, A. Camões, L. Bragança, and F. G. Branco, "Comparative Environmental Life-Cycle Analysis of Concretes Using Biomass and Coal Fly Ashes as Partial Cement Replacement Material," *J Clean Prod*, vol. 112, pp. 2221–2230, 2016, doi: 10.1016/j.jclepro.2015.09.124.
- [2] N. M. Sigvardsen, G. M. Kirkelund, P. E. Jensen, M. R. Geiker, and L. M. Ottosen, "Impact of Production Parameters on Physiochemical Characteristics of Saw Dust Ash for Possible Utilisation in Cement-Based Materials," *Resour Conserv Recycl*, vol. 145, pp. 230–240, 2019, doi: 10.1016/j.resconrec.2019.02.034.
- [3] E. E. T. Ercan, L. Andreas, A. Ćwirzeń, and K. Habermehl-Cwirzen, "Saw Dust Ash as Sustainable Alternative Raw Material for the Production of Concrete—A Review," *Materials*, vol. 16, no. 7, p. 2557, 2023, doi: 10.3390/ma16072557.
- [4] C. Gaudreault, I. Lama, and D. Sain, "Is the Beneficial Use of Saw Dust Ash Environmentally Beneficial? A Screening-level Life Cycle Assessment and Uncertainty Analysis," *J Ind Ecol*, vol. 24, no. 6, pp. 1300–1309, 2020, doi: 10.1111/jiec.13019.
- [5] V.-A. Vu, A. Cloutier, B. Bissonnette, P. Blanchet, and J. Duchesne, "The Effect of Saw Dust Ash as a Partial Cement Replacement Material for Making Wood-Cement Panels," *Materials*, vol. 12, no. 17, p. 2766, 2019, doi: 10.3390/ma12172766.
- [6] S. Chowdhury, A. T. Maniar, and O. M. Suganya, "Strength Development in Concrete With Saw Dust Ash Blended Cement and Use of Soft Computing Models to Predict Strength Parameters," *J Adv Res*, vol. 6, no. 6, pp. 907–913, 2015, doi: 10.1016/j.jare.2014.08.006.
- [7] T. G. L. J. Bikoko, "A Cameroonian Study on Mixing Concrete With Saw Dust Ashes: Effects of 0-30% Saw Dust Ashes as a Substitute of Cement on the Strength of Concretes," *Revue Des Composites Et Des Matériaux Avancés*, vol. 31, no. 5, pp. 275–282, 2021, doi: 10.18280/rcma.310502.
- [8] A. Ekinci, M. Hanafi, and E. Aydin, "Strength, Stiffness, and Microstructure of Wood-Ash Stabilized Marine Clay," *Minerals*, vol. 10, no. 9, p. 796, 2020, doi: 10.3390/min10090796.

- [9] P. O. Awoyera, J. O. Akinmusuru, A. Dawson, J. M. Ndambuki, and N. Thom, "Microstructural Characteristics, Porosity and Strength Development in Ceramic-Laterized Concrete," *Cem Concr Compos*, vol. 86, pp. 224–237, 2018, doi: 10.1016/j.cemconcomp.2017.11.017.
- [10] A. A. Raheem, B. S. Olasunkanmi, and C. S. Folorunso, "Saw Dust Ash as Partial Replacement for Cement in Concrete," *Organization Technology and Management in Construction an International Journal*, vol. 4, no. 2, 2012, doi: 10.5592/otmcj.2012.2.3.
- [11] O. S. Ogbo, E. O. Momoh, E. E. Ndububa, O. O. Afolayan, S. Onuche, and J. O. Agada, "Scheffe's Polynomial Optimisation of Laterite Concrete Incorporating Periwinkle Shells and Coir," *KSCE Journal of Civil Engineering*, vol. 00, no. 0000, pp. 1–19, 2023, doi: 10.1007/s12205-023-0110-4.
- [12] S. O. Obam, "The Accuracy of Scheffe's Third Degree Over Second-Degree, Optimization Regression Polynomials," *Nigerian Journal of Technology*, vol. 25, no. 2, pp. 5–15, 2006, [Online]. Available: <https://www.ajol.info/index.php/njt/article/view/123369>
- [13] I. C. Attah, R. K. Etim, G. U. Alaneme, and O. Bassey, "Optimization of Mechanical Properties of Rice Husk Ash Concrete Using Scheffe's Theory," *SN Appl Sci*, 2020, doi: 10.1007/s42452-020-2727-y.
- [14] U. I. Iro, G. U. Alaneme, I. C. Attah, N. Ganasen, S. C. Duru, and B. C. Olaiya, "Optimization of Cassava Peel Ash Concrete Using Central Composite Design Method," *Sci Rep*, vol. 14, no. 1, 2024, doi: 10.1038/s41598-024-58555-0.
- [15] G. A. Akeke, C. C. Nnaji, and U. U. Udokpoh, "Compressive Strength Optimisation of Rice Husk Ash Concrete Using Scheffe's Mathematical Model," *Epitoanyag-Journal of Silicate Based and Composite Materials*, vol. 74, no. 4, pp. 129–135, 2022, doi: 10.14382/epitoanyag-jsbcm.2022.20.
- [16] A. Al-Fakih, A. Odeh, M. A. A. Mahamood, M. A. Al-Shugaa, M. A. Al-Osta, and S. Ahmad, "Review of the Properties of Sustainable Cementitious Systems Incorporating Ceramic Waste," *Buildings*, vol. 13, no. 8, p. 2105, 2023, doi: 10.3390/buildings13082105.
- [17] K. Arroudj, S. Dorbani, M. N. Oudjit, and A. Tagnit-Hamou, "Use of Algerian Natural Mineral Deposit as Supplementary Cementitious Materials," *International Journal of Engineering Research in Africa*, vol. 34, pp. 48–58, 2018, doi: 10.4028/www.scientific.net/jera.34.48.
- [18] J. Fagerström, I.-L. Näzelius, C. Gilbe, D. Boström, M. Öhman, and C. Boman, "Influence of Peat Ash Composition on Particle Emissions and Slag Formation in Biomass Grate Co-Combustion," *Energy & Fuels*, vol. 28, no. 5, pp. 3403–3411, 2014, doi: 10.1021/ef4023543.
- [19] E. E. Ndububa, "Concrete From Alternative and Waste Materials," 2022, doi: 10.5772/intechopen.1000571.
- [20] R. Raja and V. Ponmalar, "Strength and Microstructural Behavior of Concrete Incorporating Laterite Sand in Binary Blended Cement," 2020, doi: 10.7764/rdlc.19.3.422-430.